ORIGINAL ARTICLE

Batch studies of turquoise blue dye (TB) adsorption onto activated carbon prepared from low-cost adsorbents: an ANN approach

Pamila Ramesh[1,2] · Vasanthi Padmanabhan[1] 🔘 · Praveen Saravanan[3] · Bhagavathi Pushpa Thillainayagam[4]

Abstract

Pumpkin peel (*Cucurbita pepo L.*) and bracts of plantain flower (*Musa acuminate*) are cellulosic and bio-degradable agricultural wastes available in abundance. This paper is aimed at assessing their potential as adsorbents by modifying into activated carbon for the adsorption of turquoise blue dye (TB). The performance was evaluated by altering the adsorption parameters such as pH, dosage, temperature, and initial dye concentration. The batch adsorption experiments were carried out with a fixed RPM and suitable contact time with different temperature ranges. The adsorbents were characterized using FTIR and SEM techniques. Adsorption isotherm study was also carried out. Adequate samples were withdrawn during the experiments to find out the concentration of dye that is adsorbed using a UV-vis spectrophotometer. From the studies, it is observed that the adsorption efficiency of pumpkin peels (PP) is higher than that of bracts of plantain flower (BP) and found to be promising alternatives for the removal of dye. Adsorption studies were modeled using Freundlich and Langmuir adsorption isotherms, and it was well fitted with Langmuir isotherm. ANN result showed that Levenberg-Marquardt (LM) algorithm was the best model bearing coefficient of regression ($R^2 = 0.9968$) and mean square error (MSE =0.00013), on the dye removal. These results are very promising and, in our opinion, establish a milestone to a vital research field.

Keywords ANN · Turquoise blue · Adsorption · Pumpkin peel · Bracts of plantain flower

1 Introduction

Dyes are used as coloring agents in various types of industries such as chemical, textile, pharmaceutical, leather, papers, and food [1]. A high amount of toxic substances generated by these industries are discharged into lakes or streams without any suitable treatment, which affects photosynthetic activity as well as groundwater quality and also leads to soil pollution [2–4].

Effluents of dyeing industries are a complex variable mixture of many polluting substances, which induce organic load and color which tends to destroy the total ecosystem in surface water bodies. Direct disposal of these effluents provoke severe environmental problems and inhibit many metabolic reactions [5]. If this pollution continues, then the surface water quality goes to the level at which it will not be used for any purpose. So under this situation, it has become urgent to think of an alternative.

Currently, the major methods used for treating dye containing textile wastewaters are physical and chemical processes such as chemical precipitation, air stripping, oxidation, flocculation, sedimentation, ion exchange, and adsorption. Among the above techniques, adsorption is considered to be most preferred owing to its effectiveness towards the removal of toxic pollutants [6]. Adsorption by activated carbon is useful in wastewater treatment, but its high cost limits its usage [7, 8]. Hence, it is necessary to search for comparatively alternate low-cost natural adsorbents from waste materials. Recently, agricultural by-products were identified as economical and efficient adsorbents for the removal of different kinds of pollutants [9]. Previous studies were done by using numerous agricultural wastes such as sugarcane bagasse [10],

✉ Vasanthi Padmanabhan
vasanthi@crescent.education; vasanthicresent@gmail.com

1 Department of Civil Engineering, School of Infrastructure, B.S. Abdur Rahman Crescent Institute of Science & Technology, Chennai, Tamil Nadu 600 048, India

2 Department of Civil Engineering, Sri Sairam Engineering College, Chennai, Tamil Nadu 600 044, India

3 Department of Civil Engineering, GMR Institute of Technology, Rajam, Andhra Pradesh 532 127, India

4 Department of Civil Engineering, Anna University, University College of Engineering Ramanathapuram, Ramanathapuram, Tamil Nadu 623 513, India

tomato plant root [11], sugar beet pulp [12], pineapple leaf powder [13] date stone, palm trees [14], water hyacinth [15], banana stalk waste [16] Indian rosewood sawdust [17], commercial activated carbon [18] and granular kohlrabi peel [19], Curcuma longa [20], Manikara zapota [21], princess tree leaf [22], coir pith [23], almond shell [24], peach stone [25], and also composts of neem leaves and water hyacinth [26, 27]. The use of bracts of plantain flower and pumpkin peel for the removal of turquoise blue dye (TB) is minimal [28, 29]. Moreover, the above-said wastes do not have any economic values and are generated in abundant quantity. Therefore, the above wastes were used as alternate adsorbents for the removal of turquoise blue from aqueous solution by adsorption process.

Over a decade, artificial intelligence was widely employed in adsorption modeling studies for the understanding of interaction between different variables [30]. But there is only a few information available towards the application of ANN for the prediction of adsorption system [31]. The objectives of the present study are to examine adsorption characteristics of BP and PP powder by batch process and to assess their maximum permissible adsorption capacity using Langmuir and Freundlich isotherms and potential applications of utilizing them as low-cost adsorbents and to validate the adsorption efficiency of the above adsorbents by using ANN model.

2 Materials and methods

2.1 Preparation of adsorbate solution

TB dye, a cationic compound purchased from Merck, is used as an adsorbate. 1 g of TB dye is dissolved in 1000ml of de-ionized water to prepare a stock solution of 1000 mg l^{-1} and further diluted to make practical solutions of desired concentrations such as 100 mg l^{-1}, 80 mg l^{-1}, 60 mg l^{-1}, 40 mg l^{-1}, and 20 mg l^{-1}. Absorbance was measured with a UV-visibility spectrophotometer (SHIMADZU-DRS Kyoto-Japan) at a maximum wavelength of 663nm for turquoise blue.

2.2 Preparation of adsorbents

The domestic wastes, namely, pumpkin peels (PP) and bracts of plantain flower (BP) were collected locally, washed numerous times with double distilled water, and left sundried. Carbonization of pumpkin peels (PP) and bracts of plantain flower (BP) was carried out at a temperature of 500°C [32] in a KSL-1700X-A3 muffle furnace. The so prepared adsorbents were preserved in a container for further studies.
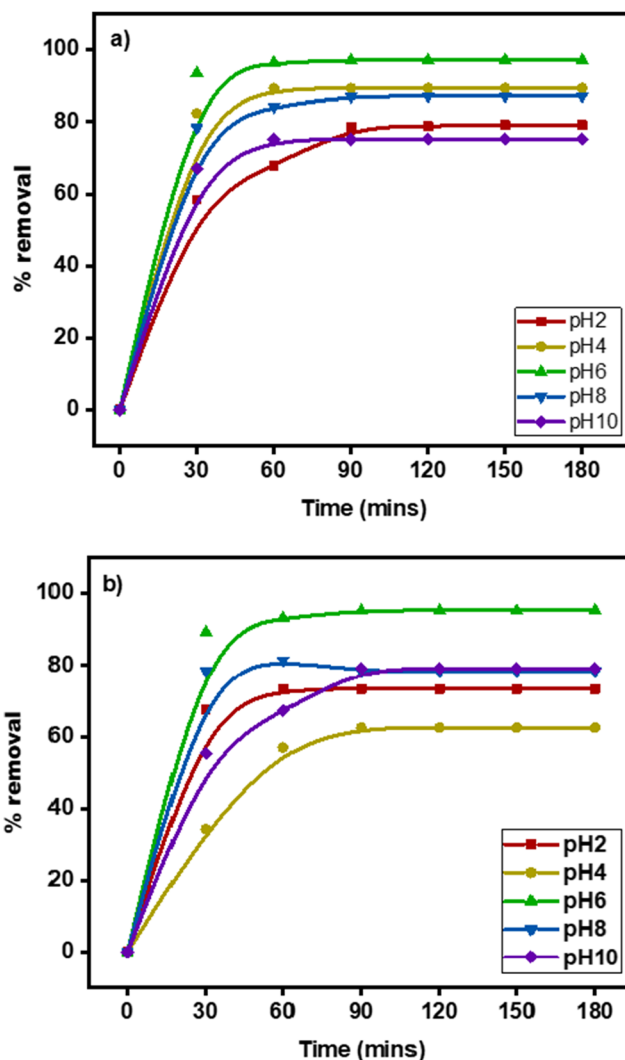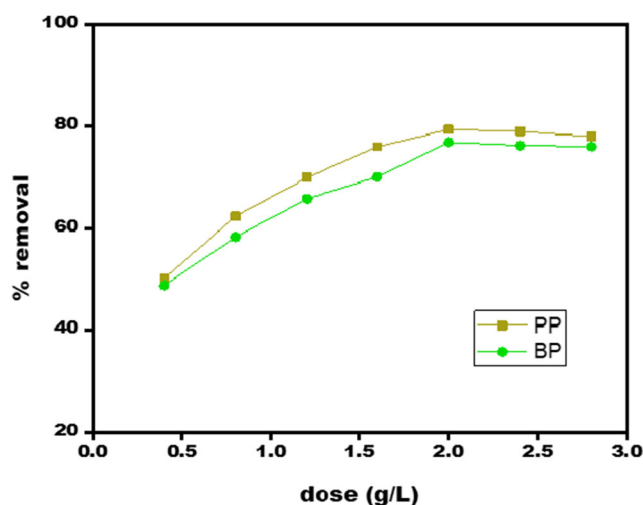
Fig. 1 Effect of pH on PP and BP

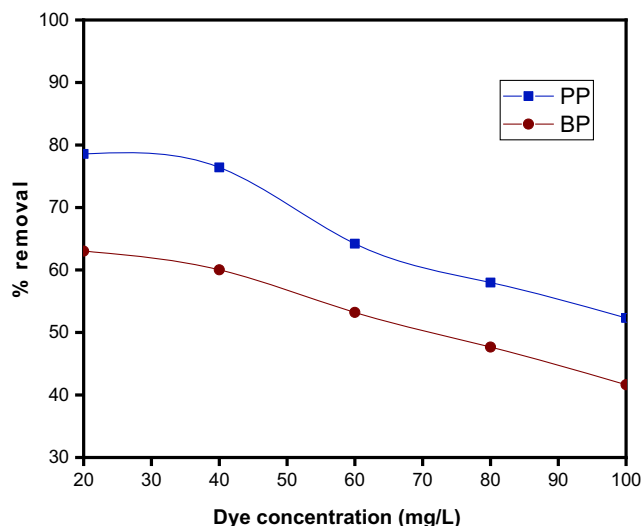Fig. 2 Effect of adsorbent dosage on to PP and BP

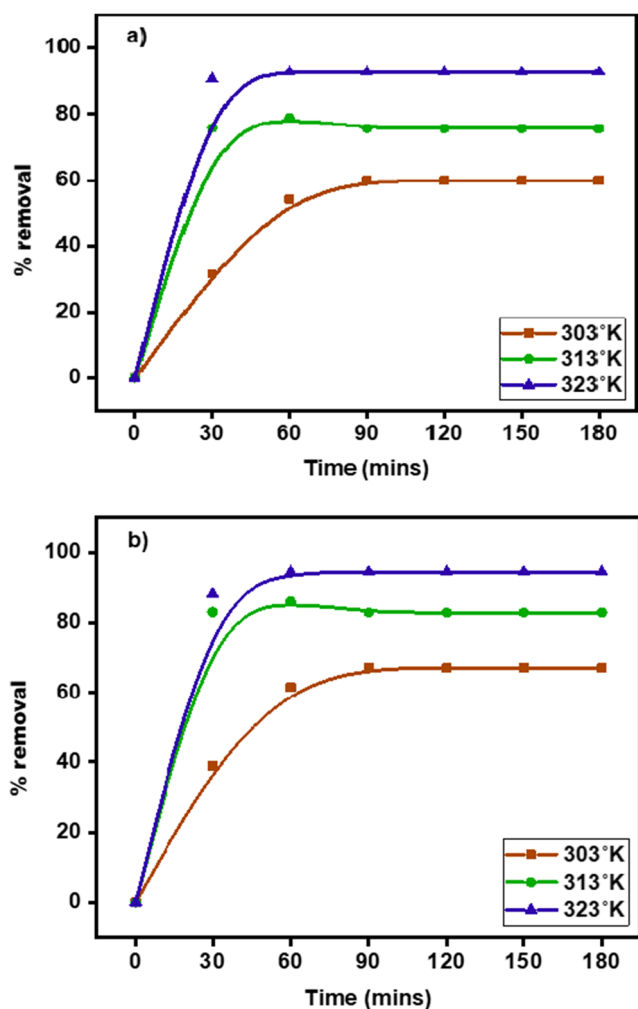Fig. 3 Effect of Initial dye concentration on PP and BP
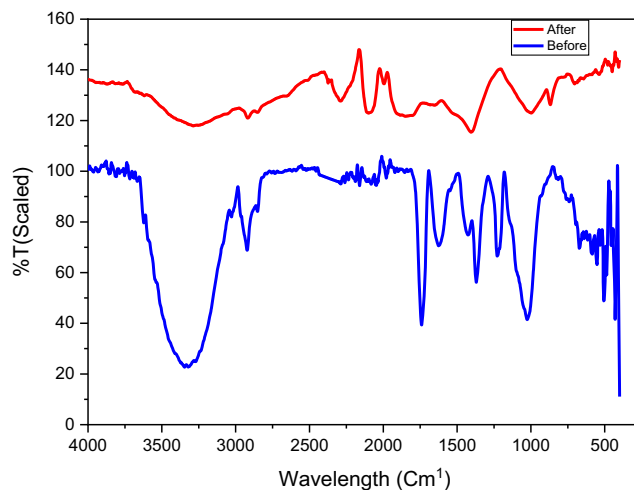

Fig. 4 Effect of temperature on (a) PP and (b) BP

Fig. 5 FTIR spectrum for PP before and after adsorption

2.3 Characterization of PP and BP

Characterization of the adsorbents PP and BP powder is done by FTIR (Thermo Nicolet, AVATAR 330 spectrometer). The Fourier transform infrared analysis reveals the information about various functional groups present in PP and BP within the range of 400-4000 cm^{-1}. The final concentration of the dye solution after filtration was measured by using a double beam UV-visibility spectrophotometer (SHIMADZU-DRS Kyoto-Japan) at a maximum wavelength of 663 nm for turquoise blue. Surface morphology of adsorbents PP and BP were studied by using a Jeol JSM 6390 scanning electron microscope (SEM).

2.4 Adsorption studies

The effects of various parameters on adsorption were determined by conducting adsorption studies in batch mode with 50 ml of turquoise blue dye medium in a 250 ml glass container containing 1g of adsorbent by varying the solution pH (2-10), adsorbent dosage (0.4 g l^{-1} to 2.0 g l^{-1}), initial dye
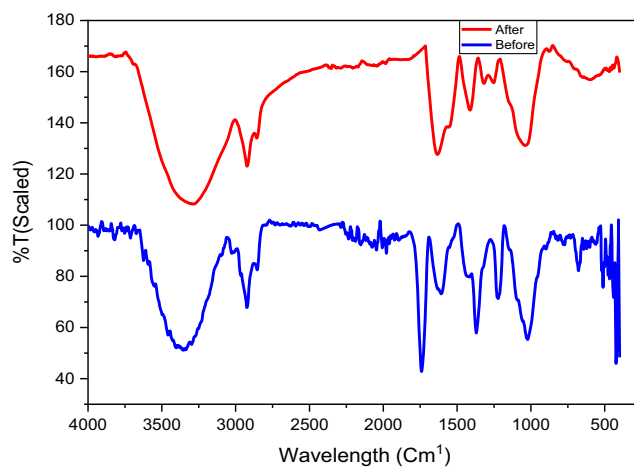

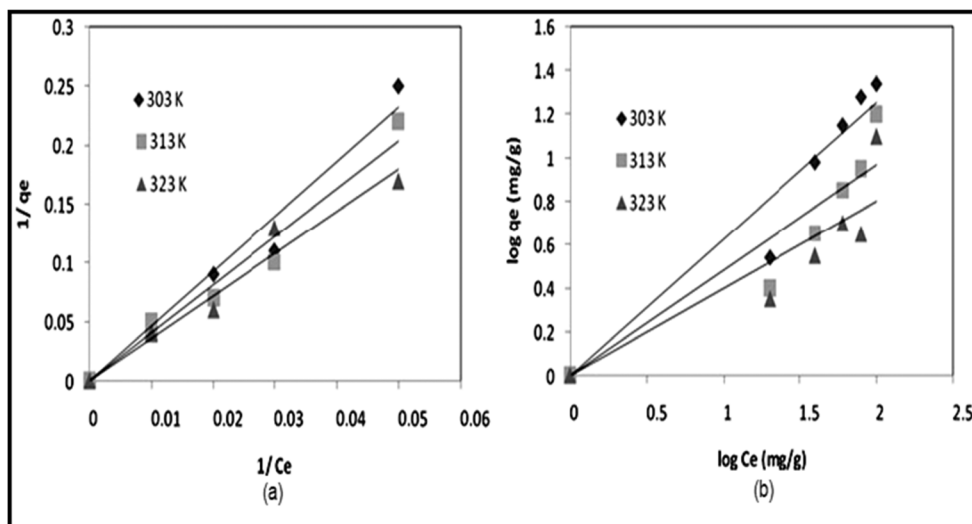Fig. 6 FTIR spectrum for BP before and after adsorption

Fig. 7 (a) Langmuir plot of TB adsorption onto PP. (b) Freundlich plot of TB adsorption onto PP

concentration (20 mgl^{-1} to 100 mgl^{-1}), and temperature (303K, 313K, and 323K) on adsorption of turquoise blue dye using pumpkin peel and bracts of plantain flower powder. By using an orbital shaker (REMI-CIS 24BL) at 300°C, the solution is kept agitated at 120rpm for 60 min. The concentrations of turquoise blue dye before and after treatment were measured using a spectrophotometer at a wavelength of 663nm. The adsorption capacity of the adsorbent and percentage removal of dye was calculated by using the relation.

$$Q_e = \frac{V(C_0 - C_e)}{m} \tag{1}$$

$$\%\text{Removal} = \left(\frac{C_0 - C_e}{C_0}\right) \times 100 \tag{2}$$

where C_0 and C_e are the initial and equilibrium concentration of the solution in mg/L, and V is the volume of adsorbate solution in m is the mass of adsorbent in g.

2.5 Isotherm and kinetic studies

The isothermal equations used in this analysis are the linear and non-linear regression methods of Freundlich and Langmuir isothermal equations. Different forms of linearized equations have been studied in Langmuir Isotherm. In the sorption process, kinetic study helps to predict the type of mechanisms involved. Lagegren's pseudo-first-order and pseudo-second-order kinetic equations were used to obtain kinetic data from the adsorption process. Biosorption energy tests were performed using a known measure of nut husk in 250 mL jars containing 50 mL color arrangements. On an orbital shaker (REMI-CIS 24BL) at

Fig. 8 (a) Langmuir plot of TB adsorption onto BP. (b) Freundlich plot of TB adsorption onto BP
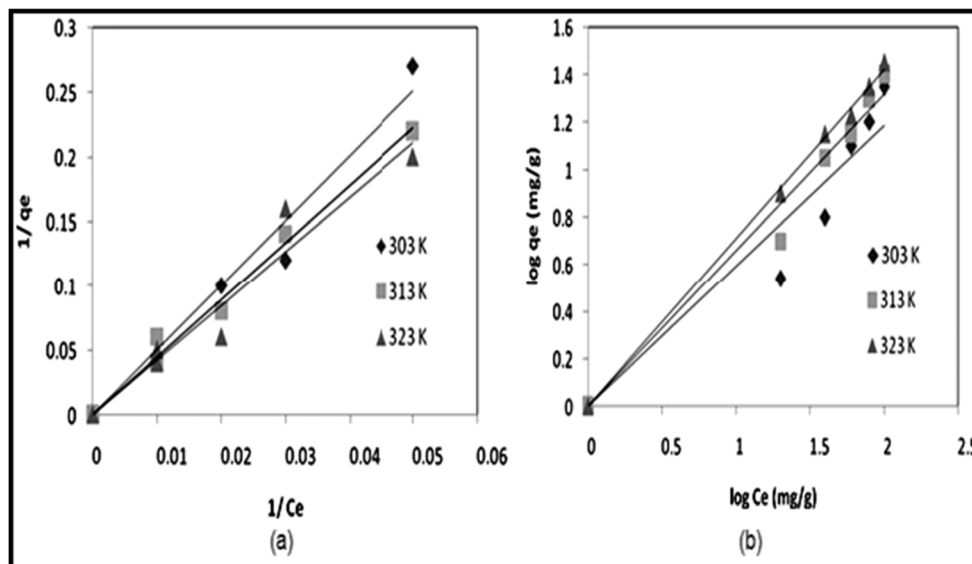
Table 1 Isotherm constants for TB adsorption onto PP

| Temperature	Langmuir isotherm parameters		
	q_m (mg/g)	K_L (L/mg)	R^2
303 K	111	0.45	0.92
313 K	140	0.68	0.95
323 K	179	0.85	0.96
	Freundlich isotherm parameters		
	K_f (mg/g) (L/g)	n	R^2
303 K	3.148	2.59	0.98
313 K	2.77	3.1	0.92
323 K	1.826	4.5	0.91

120 rpm at a steady temperature (30 °C), the jars were upset for various time stretches (0-60 min).

2.6 Artificial neural networks

A non-conventional tool for adsorption modeling that is in use for a decade or so is the ANN. ANN models have three layers, such as input, hidden, and output layers that can uptake inputs and can estimate output. ANNs are widely used nowadays due to their simplicity towards simulation, prediction, and modeling ANN's can identify and replicate root cause and consequence connections over multiple training of input and output data, even for complicated systems. ANN is of significance since it has consistent, lively, and sizeable capabilities in depicting the non-linear relationships among input and output variables in fixing complicated environmental engineering problems [31–33].
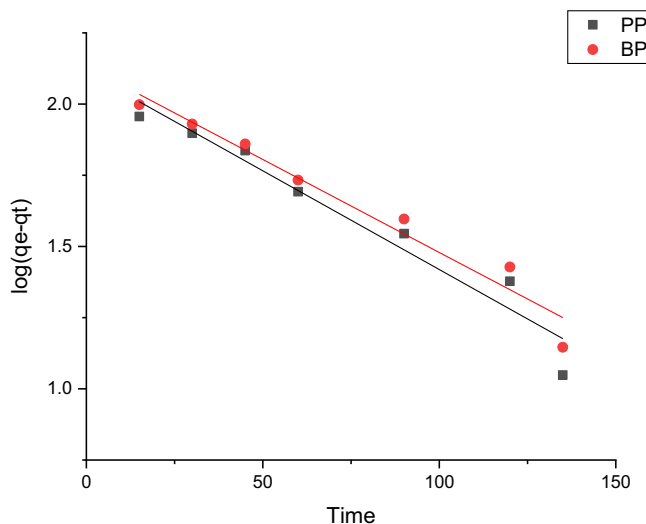
Fig. 9 First-order kinetic model for TB adsorption onto PP and BP

The estimation of TB dye from wastewaters using PP and BP is complex; hence, the artificial neural network tool was considered in this research [34]. The ANN model shown in Fig. 1, which can be used to forecast the interaction between inputs and output layers, is based on three distinct layers of input, hidden, and output layers known as neurons. The nodes are employed as neurons of ten in the hidden layer and one in the output layer. Levenberg Marquardt (LM), Bayesian regularization (BR), and Scaled Conjugate Gradient (SCG) algorithms each with 1000 iterations were employed. Regression analysis for the factors as inputs and % removal as output was performed using neural networks in MATLAB R2018b software. All of the data is divided randomly into two groups, namely, learning and testing. The data sets 70% (20), 15 % (5), and 15% (5) were used in training, validation, and testing data, which involves the input parameters pH, initial concentration, adsorbent dose, and temperature as datasets for training (70%) and others for validation and testing. The % removal is taken as output.

The findings of the study using networks and their training were compared based on mean square error (MSE) and the coefficient of determination (R^2) that are shown as:

$$MSE = 1/N \sum_{i=1}^{N} \left(\left| y_{\mathrm{pre},i} - y_{\mathrm{exp},i} \right| \right)^2$$

$$R^2 = 1 - \frac{\sum_{i=1}^{N} \left(y_{\mathrm{pre},i} - y_{\mathrm{exp},i} \right)}{\sum_{i=1}^{N} \left(y_{\mathrm{pre},i} - y_{\mathrm{avg},i} \right)} \quad (3)$$

where $y_{\mathrm{pre},i}$ and $y_{\mathrm{exp},i}$ were the predicted and the experimental values of the ANN model, N was the number of data points, and $y_{\mathrm{avg},i}$ was the average of the experimental value.

3 Results and discussion

3.1 Effect of pH

The effect of pH on adsorption of TB by the two adsorbents, namely, PP and BP powder is shown in Fig. 2a, b. The pH of the solution was altered from 2 to 10 by using 0.1N sodium hydroxide and 0.1N hydrochloric acid solution with 50 mg/l as initial dye concentration and 0.5 g/l as adsorbent dose agitated at 120 rpm at room temperature. Maximum removal efficiency was attained at pH 6 (86% for PP and 83% for BP) as at this pH the surface of the adsorbent becomes negatively charged and favors the lifting of cationic dye due to increased electrostatic forces of attraction [35, 36]. A lower removal efficiency for PP (52.45%) and BP (33%) was attained at a pH of 2. This may be due to the electrostatic

Table 2 Isotherm constants for TB adsorption onto BP

Temperature	Langmuir isotherm parameters		
	q_m (mg/g)	K_L (L/mg)	R^2
303 K	120	0.21	0.902
313 K	140	0.55	0.924
323 K	169	0.67	0.897
	Freundlich isotherm parameters		
	K_f (mg/g) (L/g)	n	R^2
303 K	3.148	1.54	0.867
313 K	2.77	1.28	0.894
323 K	1.826	1.02	0.910

repulsion between the adsorbent surface and dye molecules at lower pH and also the concentration of H^+ ions decreases as the pH value increases, which increases the number of negatively charged sites [37–39] and so there was a decrease in removal efficiency above pH 6. Therefore, TB dye removal by the adsorbents PP and BP powder are favored at pH 6. Hence, the remaining experiments were performed at this pH.

3.2 Effect of adsorbent dosage

Adsorbent dose occupied a significant role in the removal of color. The amount of adsorbent was varied from 0.4 g l^{-1} to 2 g l^{-1} by keeping pH at 6, with an optimum dye concentration of 100 mg l^{-1} under an equilibrium time of 60 min and at a temperature of 30 °C. Figure 3 depicts the effect of adsorbent dosage on dye removal. It is evident that the removal efficiency increases with an initial increase in the adsorbent dose and in case of further addition beyond optimum dosage leading to the decrease of sorption capacity [40]. As adsorption sites get overlapped/saturated, there is a reduction in sorption due to
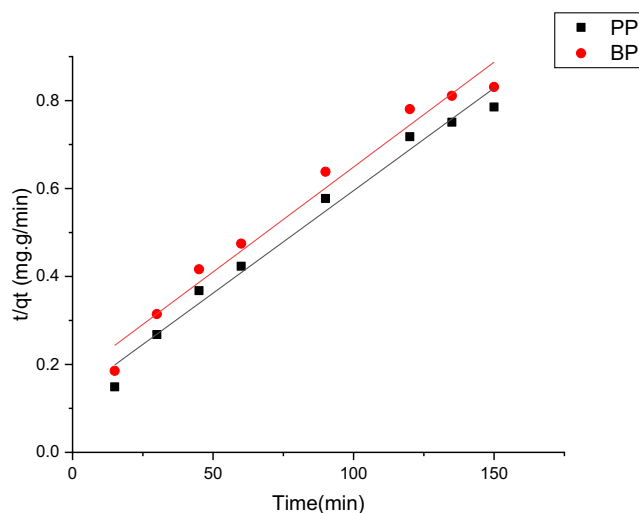
Fig. 10 Second-order kinetic model for TB adsorption onto PP and BP

less contact with the dye molecules onto the adsorbent surface [41]. The sorption capacity declined from 20.03 mg/g to 3.84 mg/g (PP) and from 18.24 mg/g to 3.5 mg/g (BP), whereas the removal efficiency increases from 50.14% to 78.8% (PP) and from 48.78% to 75.12% (BP). Comparing the percentage removal and at other dosages, the optimum adsorbent dosage for sorption is taken as 2 g l^{-1}.

3.3 Effect of initial dye concentration

Figure 4 shows the percentage removal of TB dye for PP and BP powder at different initial concentrations (20 mg l^{-1}, 40 mg l^{-1}, 60 mg l^{-1}, 80 mg l^{-1}, and 100 mg l^{-1} with contact time onto adsorbents at different time intervals from 10 min to 60 min by maintaining pH at 6 and adsorbent dose at 2 g l^{-1}. With increasing initial dye concentration, the dye uptake capacity increased and the percent removal decreased. The decrease in the percent removal of TB was evident with PP (78.57%) and BP (63.01%), at 20 mg l^{-1} and at 100 mg l^{-1}, it was observed as PP (52.32%) and BP (42%). The original number of dye molecules at the lower concentration was greater than the available surface area [42, 43]. The initial adsorption was thus independent of the dye molecules' initial concentration. However, the available surface area of the adsorbent gradually decreases at a higher concentration, and thus the dye's adsorption percentage depends on the initial dye concentration [44, 45].

3.4 Effect of temperature on PP and BP

Figure 5a, b represents the percentage removal efficiency of PP and BP at the temperature ranges 30°C (303K), 40°C (313K), and 50°C (323K), respectively. The effect of temperature on the adsorption rate of TB dye was investigated by contacting 50 mL of dye solution with 2 g l^{-1} of PP and BP. The diffusion of the adsorbate molecules is caused by a rise in the adsorbent particle's temperature leading to a reduction in the aqueous medium's viscosity. The amount of dye absorbed increased from 4.5 mg/g to 21 mg/g for PP and from 3 mg/g to 22 mg/g for BP, indicating the process is endothermic [46]. It is due to the interaction between the functional group, the particles favor adsorption at high temperature. Therefore, the variation in temperature will alter the adsorbate equilibrium capacity.

3.5 FTIR analysis

FTIR spectrum of PP before and after the adsorption process is shown in Fig. 6. Before the adsorption process of pumpkin peel powder, the peak at 3346.89 cm^{-1} represents the occurrence of amines. At 2917.7 cm^{-1} and 2853.17 cm^{-1}, the deduced peaks were due to the stretching of C-H bonds, which indicates the presence of alkanes. The peaks at 2235.09 cm^{-1}

Table 3 Kinetic parameters for adsorption of TB onto PP and BP powder

Kinetic models	Parameters	PP	BP
	q_e (mg/g)	8.281	8.431
Pseudo-first-order model	k_1 (min^{-1})	0.01598	0.01503
	R^2	0.9371	0.9529
	q_e (mg/g)	21.459	20.964
Pseudo-second-order model	k_2 (min^{-1})	1.6×10^{-4}	1.25×10^{-4}
	R^2	0.979	0.9709

indicate the presence of nitrile. The decreasing intensity of peaks between 1739.48 cm^{-1} shows the presence of alkynes. After the adsorption process, the peaks shown at 3767.26 cm^{-1} shows the presence of alcohol and at 2917.77cm^{-1} shows the presence of alkanes by the stretching of the C-H bond. The peak 2373.94cm^{-1} and 2289.09 cm^{-1} indicate the nitrile group. 2100.1cm^{1}, 1996cm^{-1}, and 1849.4cm^{-1} indicate alkynes and aromatics group.

From Fig. 7, which shows the FTIR spectrum for BP before and after adsorption with TB dye solution, it can be deduced that the peak at 3624.55 cm^{-1} represents the occurrence of alcohol by the stretching of O-H. The N-H stretching at 3355.53 cm^{-1} indicates amines, alkanes, and nitrile were at 2923.56 cm^{-1} and 2431.8cm^{-1}. The peak at 2187.85 cm^{-1} attributes to alkynes. After the adsorption process, the peak at 2922.02 cm^{-1} represents alkanes responsible for stretching of the C-H bond at 2867.02cm^{-1}. The peak at 2206.17cm^{-1} shows the nitrile group. These functional groups play a major role in the adsorption of turquoise blue dye on to the bracts of plantain flower powder particles.
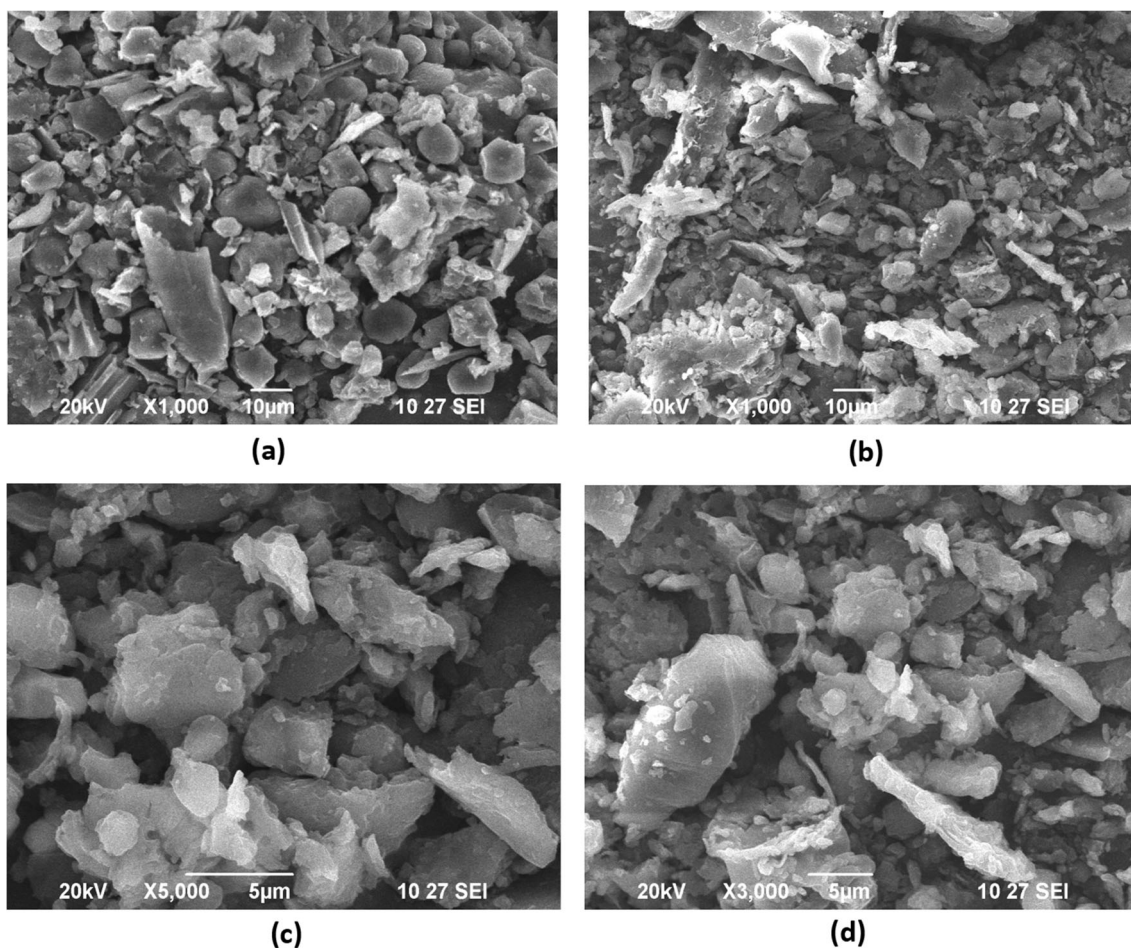
Fig. 11 SEM analysis for (a) PP powder before adsorption, (b) PP powder after adsorption, (c) BP powder before adsorption, and (d) BP powder after adsorption
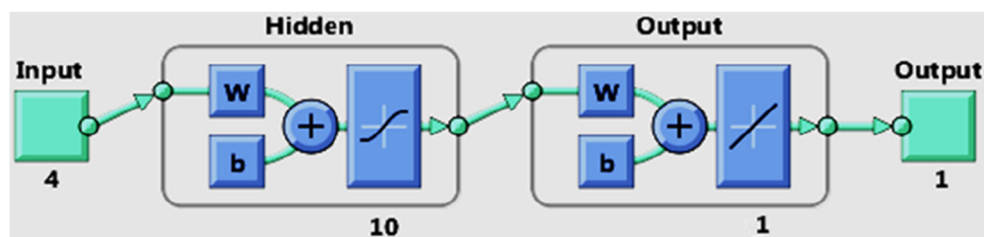
Fig. 12 ANN architecture for LM, BR, and SCG algorithms

3.6 Adsorption isotherms

In the design of adsorption systems, adsorption isotherm is of significance and also to understand the optimization of process conditions. The relationship between the adsorbate and the adsorbent in the solution is described as an isotherm. Two important isotherms selected in this study are the Freundlich and Langmuir isotherms for a deeper interpretation of the adsorption data obtained. The equilibrium data in the dye concentration of 50 mg l^{-1}, optimum pH at 6, and temperature varying at 303K, 313K, and 323K were fit into the isotherms. The below-mentioned isotherm expression examined the equilibrium data with the help of the following equations.

Langmuir isotherm

$$qe = 1 + \frac{q_{m\,K_L\,C_e}}{K_L C_e} \qquad (4)$$

Freundlich isotherm

$$q_e = K_f C_e^{1/n} \qquad (5)$$

In Langmuir isotherm, q_m is the maximum sorption capacity (mg/g), and K_L is the Langmuir constant correlated to the energy of adsorption (L/mg). The Langmuir constants q_m and K_L were calculated from the slope of the plot between $1/q_e$ versus $1/C_e$. The Langmuir isotherm assumes that the surface of the adsorbents having homogenous binding sites with equal adsorption capacity lies in a single layer [47].

Where K_f (mg/g) and n are Freundlich constants linked to adsorption capacity and intensity of adsorbents, q_m is the maximum sorption capacity (mg/g). The Freundlich constants K_f and n were calculated from the intercept and slope of the plot between log q_e and log C_e.

Figure 8a, b represents the Langmuir and Freundlich plots for TB dye onto Pumpkin peel powder at a constant temperature of 30°C (303K), 40°C (313K), and 50°C (323K). The experimental results thus obtained were analyzed using the Freundlich and Langmuir isotherm. It is evident that the equilibrium data is well fitted with the Langmuir isotherm than compared to the Freundlich isotherm model. The sorption isotherm constants for TB adsorption onto PP along with correlation coefficients, R^2 values are listed in Table 1.

Figure 9a, b represents the Langmuir and Freundlich curves for TB adsorption onto BP powder. The plots indicate that the data satisfies Langmuir isotherm better than Freundlich isotherm. That is because of the application of Langmuir isotherm that every site of adsorption is equal and that a particle's ability to bind there is independent of whether the neighboring sites are occupied or not and after a layer of adsorbate molecules is established on the adsorbent surface, the adsorbent is saturated. Equilibrium isotherm constants for TB dye adsorption onto BP along with correlation coefficients, R^2 values are shown in Table 2.

3.7 Kinetics of adsorption process

To choose optimum operating conditions for design purposes, the kinetics of adsorbate uptake is significant. The adsorption kinetics mainly explains the adsorbate uptake rate and regulates the residual time of the entire process of adsorption [48]. The adsorption mechanism and potential rate control steps such as chemical reaction, diffusion control, and mass transport process are investigated using kinetic models. Two kinetic models viz, pseudo-first-order, and pseudo-second-order models, were used to evaluate the experimental results in the present analysis. The sorption kinetics were carried out at a temperature of 323K, pH of 6, and 50 mg l^{-1} of TB on an adsorbent dose of 2 g l^{-1} for 60mins.

3.7.1 Pseudo-first-order kinetic model

For lower concentration of the pseudo-first-order kinetic model of Lagergren is more suitable [49] and the linear form of Lagergren eqn. is

$$\log(qe-qt) = \log qe - \frac{k_1}{2.303} t \qquad (6)$$

Table 4 MSE and R^2 for LM, BR, and SCG algorithms

Algorithm	Samples			MSE	R^2
	Training	Validation	Testing		
LM	20	5	5	0.00013	0.9968
BR	20	5	5	0.1354	0.6646
SCG	20	5	5	0.0782	0.7054

where q_e and q_t (mg/g) are the adsorption capacities at equilibrium at time t, respectively, k_1 (min^{-1}) is the rate constant of the pseudo-first-order model. The rate constant k_1 and q_e values can be obtained from the plot of log (q_e-q_t) versus time shown in Fig. 10, and the constants are given in Table 3.

3.7.2 Pseudo-second-order kinetic model

The second-order kinetic model expresses the kinetics of adsorption by the following linear equation:

$$\frac{t}{q_t} = \frac{1}{k_2 q_e^2} + \frac{t}{q_e} \qquad (7)$$

The second-order rate constant k_2 (g/mg. min-1) and q_e values are calculated from the slope and intercept of the linear plots of t/q_t vs. t shown in Fig. 11, respectively, and the constant values are given in Table 3. The values show that in contrast to the plot of a pseudo-first-order model, the plot of the second-order model yields straight lines. It is also clear from the correlation coefficients (R^2) that for the adsorption process the second-order kinetic model is followed.

3.8 Scanning electron microscope analysis

The surface morphological functionalities of the activated carbon derived from pumpkin peel and bracts of plantain flower
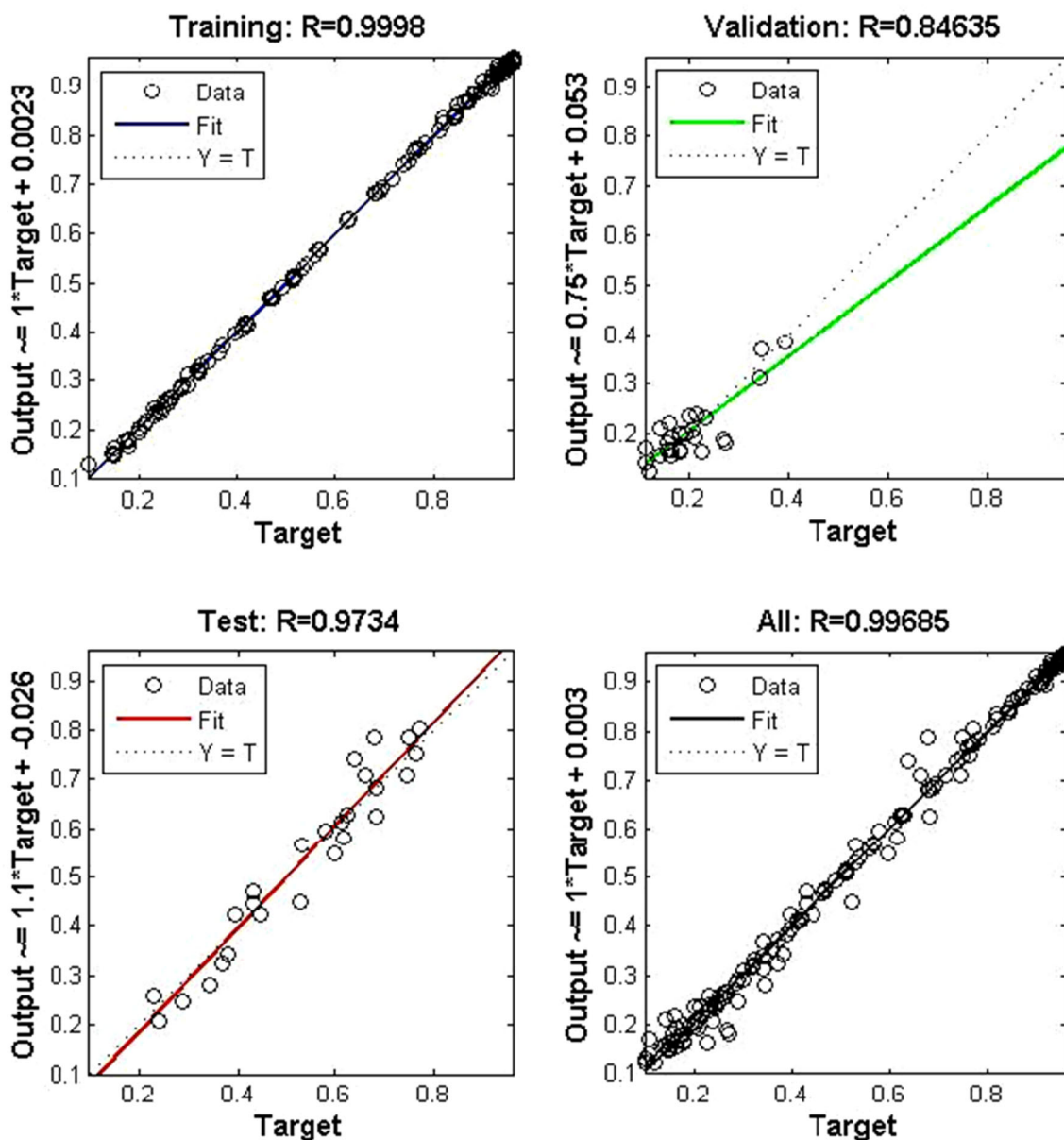

Fig. 13 Regression for LM algorithm

powder before and after the adsorption process were analyzed by the scanning electron microscope, as shown in Fig. 12a–d. SEM analysis was done for the two adsorbents to study its morphology during the adsorption process. PP and BP powders have a significant number of heterogeneous pores for the dye to be captured and adsorbed. It is clear that the surface of PP and BP is covered with a layer of dye [50].

3.9 Artificial neural network (ANN)

ANN modeling studies were performed using MATLAB R2018 b software. ANN model has three layers, such as input layer (independent variables), hidden, and output layers (dependent variables) that can uptake inputs and can estimate output. The architecture of the network employed is shown in Fig. 1. ANNs are widely used nowadays due to their simplicity towards simulation, prediction, and modeling. ANNs can identify and replicate root cause and consequence connections over multiple training of input and output data, even for complicated systems. The hidden and output layers had interconnected elements called neurons and are ten and one in

numbers. pH, initial concentration, adsorbent dosage, and temperature were used as input parameters of the neural network to predict the removal efficiency as output. The regression parameters for each case were predicted in training, testing, and validation, respectively.

Levenberg-Marquardt (LM), Bayesian regularization (BR), and Scaled Conjugate Gradient (SCG) algorithms each with 1000 iterations were employed. Regression analysis for the factors as inputs and % removal as output was performed using neural networks in MATLAB R2018b software. The architecture of the three (input, hidden, and output) layered network employed is shown in Fig. 1. LM, BR, and SCG algorithms each with 1000 iterations were employed. 30 data sets obtained from experiments were used in this study. Out of 30 data sets, 70% (20), 15 % (5), and 15% (5) samples were used in training, validation, and testing the data.

The findings of the study using networks and their training were compared based on mean square error (MSE) and the coefficient of determination (R^2) that are shown as:

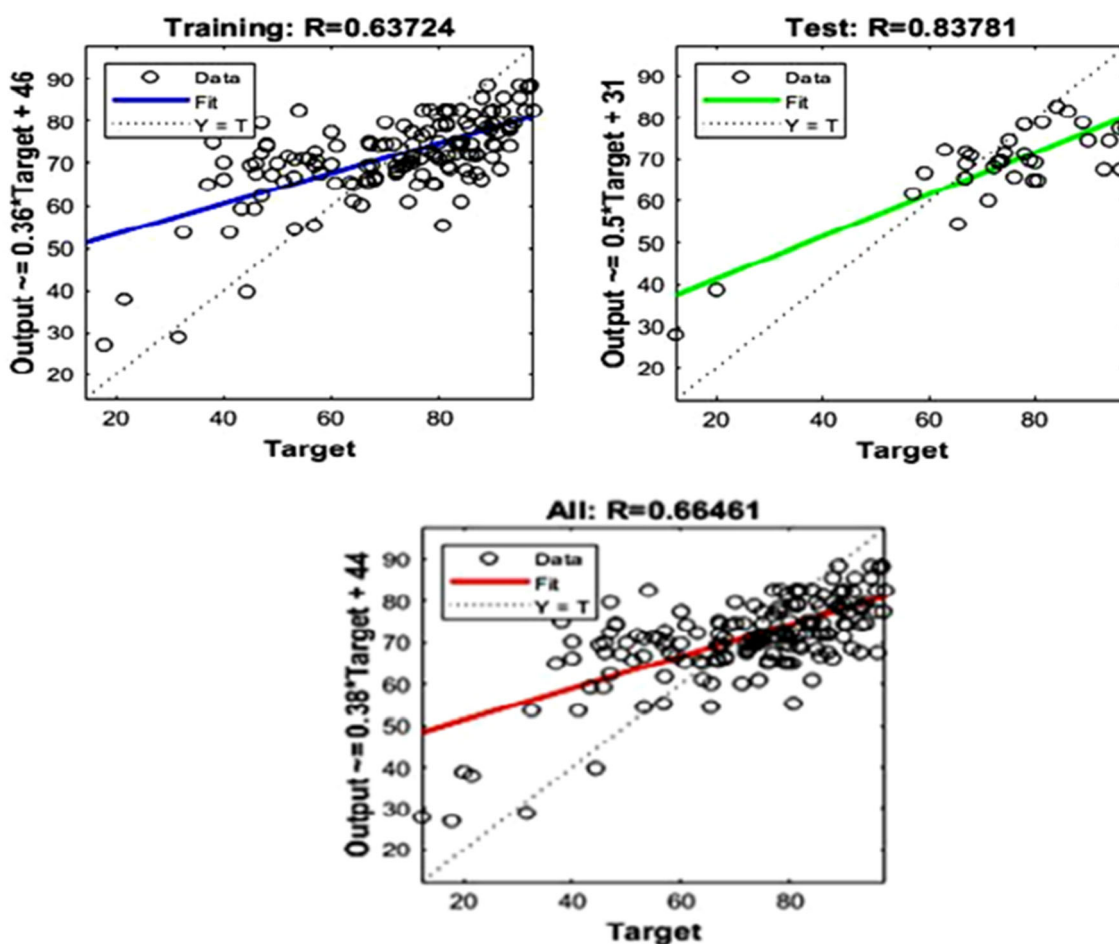$$MSE = 1/N \sum_{i=1}^{N} \left(\left| y_{\text{pre},i} - y_{\text{exp},i} \right| \right)^2 \tag{8}$$

Fig. 14 Regression for BR algorithm

$$R^2 = 1 - \frac{\sum_{i=1}^{N}\left(y_{\text{pre},i} - y_{\text{exp},i}\right)}{\sum_{i=1}^{N}\left(y_{\text{pre},i} - y_{\text{avg},i}\right)} \qquad (9)$$

where $y_{\text{pre},i}$ and $y_{\text{exp},i}$ were the predicted and the experimental values of the ANN model, N was the number of data points, and $y_{\text{avg},i}$ was the average of the experimental value.

The best regression parameters and MSE that were given in Table 4 show that LM has the least MSE among the three algorithms. Figures 13, 14, 15 show the regression plots for LM, BR, and SGR algorithms. Also, it is evident from Table 4 that the regression value ($R^2 = 0.9968$) for the LM algorithm was more suitable for the current study. The experimental and predicted dye removal (%) on PP and BP were given in Table 5.

As shown in the Fig. 13 models for training, validation, and testing of 30 datasets in the LM algorithm, the ANN model obtained a good relationship from the training data for optimized structure and performed reasonably well in validation and testing, although there is some dispersion of data. Overall, the ANN model performed satisfactorily in the experimental dataset for batch adsorption.

3.10 Thermodynamic studies

Thermodynamic studies were carried out in order to determine the conditions of equilibrium and spontaneous processes, and the thermodynamic parameters such as the change in enthalpy (ΔH^0), change in entropy (ΔS^0), and change in free energy (ΔG^0) values were calculated from the following relations.
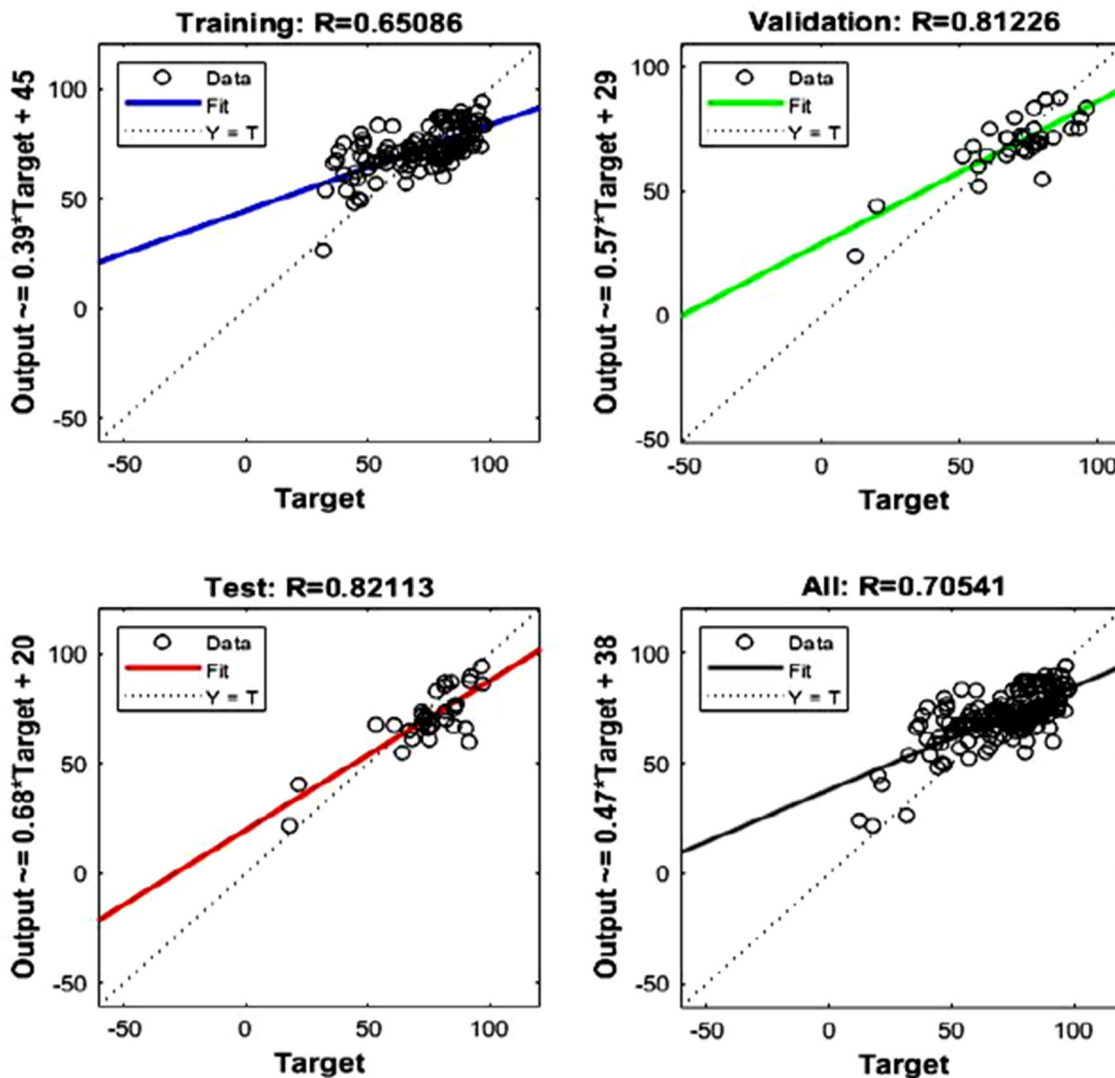
$$\Delta G° = -RT \ln K_L \qquad (10)$$

Fig. 15 Regression for SCG algorithm

Table 5 Experimental and predicted removal (%) using ANN (LM)

Run no.	pH	Initial conc. (mg/L)	Adsorbent dose (gm/L)	Temp. (K)	Removal time (min)	Removal with PP (%)		Removal with BP (%)	
						Exp	Pre	Exp	Pre
Training									
1	2	20	0.4	303	30	60.71	59.11	64.55	66.12
2	2	40	0.8	313	30	67.87	63.65	76.55	77.34
3	2	60	1.2	323	30	70.19	70.11	50.27	52.33
4	4	40	0.8	303	60	45.65	41.34	56.43	56.98
5	4	40	1.6	313	60	33.76	44.87	68.32	68.75
6	4	60	2.0	303	60	66.31	67.21	45.31	46.87
7	4	80	2.0	323	60	75.29	71.11	51.67	54.33
8	6	100	2.0	303	60	87.44	89.23	79.98	80.35
9	6	80	0.4	303	60	79.23	83.56	78.67	76.34
10	6	60	0.8	313	60	75.15	78.90	67.32	68.74
11	6	20	1.2	313	30	54.34	53.23	45.03	45.34
12	6	100	2.0	323	60	81.34	81.45	85.14	85.32
13	8	20	0.4	303	60	75.35	73.33	79.34	78.09
14	8	40	0.4	303	60	69.34	71.56	66.43	65.34
15	8	60	0.8	313	60	45.87	48.30	56.17	45.23
16	8	80	1.6	323	60	54.87	57.64	64.12	62.64
17	10	60	1.6	303	60	60.12	58.30	58.33	57.24
18	10	80	1.2	313	60	64.31	64.45	61.35	60.54
19	10	100	0.8	323	60	47.56	57.65	44.93	44.15
20	10	20	0.4	303	30	51.38	48.95	57.78	56.83
Testing									
1	4	20	0.8	303	30	63.21	67.55	78.37	76.36
2	6	40	2.0	303	60	89.54	92.45	88.58	85.34
3	6	60	2.0	313	60	78.32	78.44	81.60	81.34
4	6	80	0.4	323	45	67.87	67.22	64.43	65.12
5	8	40	1.2	303	30	56.09	55.34	47.06	47.21

$$\Delta G° = \Delta H° - T\Delta S° \qquad (11)$$

$$\ln K_L = -\frac{\Delta H°}{RT} + \frac{\Delta S°}{R} \qquad (12)$$

where R is the universe gas constant (8.314×10^{-3} KJ mol^{-1}k), K_L is Langmuir constant at a temperature T.

The values of ΔH^0 and ΔS^0 can be calculated from the slope and the intercept of the plot of $\ln K_L$ versus $1/T$ and the values obtained are given in Table 6.

From the table, it is seen the negative values of free energy change (ΔG^0) indicate the nature of the adsorption process is spontaneous [51]. Also, the ΔG^0 values decrease with the increase in temperature showing the favorability of the adsorption process at higher temperatures. The positive value

of entropy change (ΔS^0) shows there is an increase in randomness during adsorption of TB onto PP and BP [52, 53]. The reaction is endothermic indicated by positive value of change in enthalpy (ΔH^0).

4 Conclusion

The following conclusions are derived from the study,

(1) The activated carbon obtained from the agricultural residues such as pumpkin peel (PP) and bracts of plantain flower (BP) powder could be used as potential adsorbents for the removal of turquoise blue (TB) dye from aqueous solutions

(2) The SEM analysis exhibits the presence of rough and porous structure on the surface and FTIR confirms the main functional groups present on the surface of the adsorbents responsible for the adsorption process

(3) The highest removal efficiency was achieved at the optimum parameters at pH of 6, adsorbent dosage of 2 g l^{-1}, initial dye concentration of 100 mg l^{-1}, at a contact time of 60 mins, and temperature being at 323Km, and it is concluded that PP is a better adsorbent on comparing with BP

Table 6 Thermodynamic parameters for adsorption of TB onto PP and BP powder

Adsorbent	$\Delta H°$ (KJ/mol)	$\Delta S°$ (J/mol/k)	$\Delta G°$ (KJ/mol)		
			303K	313K	323K
PP	6.16	27.82	-2.257	-2.565	-2.812
BP	7.73	32.23	-1.997	-2.435	-2.637

(4) The experimental results showed a better fit with Langmuir isotherm than Freundlich isotherm. And the Kinetics of adsorption followed pseudo-second-order model than pseudo-first-order model

(5) ANN was considered to be an effective model for explaining the adsorption mechanism of TB dye onto PP and BP because of the lower MSE and higher R^2 between the predicted and experimental data

(6) From results of the temperature effect and thermodynamic studies revealed that the process is endothermic, spontaneous, and physio-sorption

References

1. Fan L, Zhang Y, Luo C, Lu F, Qiu H, Sun M (2012) Synthesis and characterization of magnetic-cyclodextrin–chitosan nanoparticles as nano-adsorbents for removal of methyl blue. Int J Biol Macromol 50:444–450. https://doi.org/10.1016/j.ijbiomac.2011.12.016

2. Jegan J, Praveen S, Bhagavathi Pushpa T, Gokulan R (2020) Sorption kinetics and isotherm studies of cationic dyes using groundnut (Arachis hypogaea) shell derived biochar a low-cost adsorbent. Appl Ecol Environ Res 18(1):1925–1939. https://doi.org/10.15666/aeer/1801_19251939

3. Saravanan P, Thillainayagam BP, Ravindiran G, Josephraj J (2020) Evaluation of the adsorption capacity of Cocos Nucifera shell derived biochar for basic dyes sequestration from aqueous solution. Energy Sources, Part A Recov Util Environ Effects:1–17. https://doi.org/10.1080/15567036.2020.1800142

4. Tanzifi M, Hosseini SH, Kiadehi AD, MartinOlazar KK, Rezaiemehr R, Al I (2017) Artificial neural network optimization for methyl orange adsorption onto polyaniline nano-adsorbent: kinetic, isotherm and thermodynamic studies. J Mol Liq 244:189–200. https://doi.org/10.1016/j.molliq.2017.08.122

5. Roushdy H, Guendy (2010) Treatment and reuse of wastewater in the textile industry by means of coagulation and adsorption techniques. J Appl Sci Res 6:964–972

6. El-Darsa FMSE, Ibrahima MA, Gabr AME (2013) Reduction of COD in water-based paint wastewater using three types of activated carbon. Desalin WaterTreat 52:2975–2986. https://doi.org/10.1080/19443994.2013.804456

7. Vunain E, Kenneth D, Biswick T (2017) Synthesis and characterization of low-cost activated carbon prepared from Malawian baobab fruit shells by H3PO4 activation for removal of Cu(II) ions: equilibrium and kinetics studies. Appl Water Sci 7:4301–4319. https://doi.org/10.1007/s13201-017-0573-x

8. Kayoed A, Bello A, Olugbenga (2015) Dye sequestration using agricultural wastes as adsorbents. Water Resour Indust 12:8–24. https://doi.org/10.1016/j.wri.2015.09.002

9. Silva NCG, Souza MCM, Jr Silva IJ, dos Santos ZM, Rocha MVP (2015) Removal of reactive turquoise blue dye from aqueous solution using a non-conventional natural adsorbent. Sep Sci Technol 50(11):1616–1628. https://doi.org/10.1080/01496395.2014.988829

10. Azhar SS, Liew AG, Suhardy D, Hafiz KF, Hatim MDI (2005) Dye removal from aqueous solution by using adsorption on treated sugarcane bagasse. Am J Appl Sci 2(11):1499–1503. https://doi.org/10.3844/ajassp.2005.1499.1503

11. Kannan C, Buvaneswari N, Palvannan T (2009) Removal of plant poisoning dyes by adsorption on tomato plant root and green carbon from aqueous solution and its recovery. Desalination 249:1132–1138

12. Vučurović, Vesna VV, Radojka R, Miodrag T (2012) Methyl blue (cationic dye) adsorption onto sugar beet pulp: equilibrium isotherm and kinetic studies. J Taiwan Inst Chem Eng 43:108–111. https://doi.org/10.1016/j.jtice.2011.06.008

13. Kamaru AA, Sani NS, Malek NANN (2016) Raw and surfactant-modified pineapple leaf as adsorbent for removal of methylene blue and methyl orange from aqueous solution. Desalin Water Treat 57(40):18836–18850. https://doi.org/10.1080/19443994.2015.1095122

14. Belala Z, Jeguirim M, Belhachemi M, Addoun F, Trouvé G (2011) Biosorption of basic dye from aqueous solutions by date stones and palm-trees waste: kinetic, equilibrium and thermodynamic studies. Desalination 271:80–87

15. Boonpoke A (2015) Study on preparation of water hyacinth-based activated carbon for pulp and paper mill wastewater treatment. J Environ Biol 36:1143–1148

16. Hameed BH, Mahmoud DK, Ahmad AL (2008) Sorption equilibrium and kinetics of basic dye from aqueous solution using banana stalk waste. J Hazard Mater 158:499–506

17. Garg V, Amita K, Kumar R, Gupta R (2004) Basic dye (turquoise blue) removal from simulated wastewater by adsorption using Indian rosewood sawdust: a tiTBer industry waste. Dyes Pigments 63:243–250

18. Maurya N, Mittal AK, Cornel P (2008) Evaluation of adsorption potential of adsorbents: a case of uptake of cationic dyes. J Environ Biol 29:31–36

19. Gong R, Zhang X, Liu H, Sun Y, Liu B (2007) Uptake of cationic dyes from aqueous solution by biosorption onto granular kohlrabi peel. Biores.Techol. 98:1319–1323

20. Roopavathi KV, Shanthakumar S (2016) Adsorption capacity of Curcumalongafor the removal of basic green1 dye – equilibrium, kinetics and thermodynamic study. J Environ Biol 37:979–984

21. Sundararaman B, Muthuramu KL (2016) A comparison of Mango seed kernel powder, mango leaf powder and Manikara zapota seed powder for decolorization of turquoise blue dye and antimicrobial activity. J Environ Biol 37:1315–1321

22. Deniz F, Saygideger S (2011) Removal of a hazardous azo dye (Basic Red 46) from aqueous solution by princess tree leaf. Desalination 268:11

23. Kavitha D, Namasivayam C (2007) Experimental and kinetic studies on turquoise blue adsorption by coir pith carbon. Bioresour Technol 98:14–21

24. Ardejani D, Badii N, YousefiLimaee SZ, Shafaei AR (2008) Mirhabibi: Adsorption of Direct Red 80 dye from aqueous solution onto almond shells: effect of pH, initial concentration and shell type. J Hazard Mater 151:730–737

25. Saratale RG, Sivapathan SS, W JJ, Kim HY, Saratale GD, Kim DS (2016) Preparation of activated carbons from peach stone by HPO activation and its application for the removal of Acid Red 18 and dye containing wastewater. J Environ Sci Health Part A 51:164–177

26. Bhagavathi Pushpa T, Jegan J, Praveen S, Gokulan R (2019) 'Biodecolorization of basic blue 41 using EM based composts: isotherm and kinetics. Chem Select 4(34):10006–10012. https://doi.org/10.1002/slct.201901774

27. Thillainayagam BP, Saravanan P, Ravindiran G et al (2021) Continuous sorption of methylene blue dye from aqueous solution using effective microorganisms-based water hyacinth waste compost in a packed column. Biomass Conv Bioref. https://doi.org/10.1007/s13399-020-01208-9

28. Rashid J, Tehreem F, Rehman A, Kumar R (2019) Synthesis using natural functionalization of activated carbon from pumpkin peels

for decolourization of aqueous methylene blue. Sci Total Environ 671:369–376. https://doi.org/10.1016/j.scitotenv.2019.03.363

29. Padmaja M, Pamila R (2017) Comparative study of low cost adsorbents in the elimination of methylene blue dye from aqueous solutions. Int J Adv Res Ideas Innov Technol 3(3):1396–1401

30. Kavitha B, Sarala Thambavani D (2016) Kinetics, equilibrium isotherm and neural network modeling studies for the sorption of hexavalent chromium from aqueous solution by quartz/feldspar/wollastonite. RSC Adv 6(7):5837–5847

31. Coruh S, Gürkan HE, Kilic E, Geyikci F (2014) Prediction of adsorption efficiency for the removal malachite green and acid blue 161 dyes by waste marble dust using ANN. Global NEST J 16(4):676–689

32. Hendrawan Y, Sajidah N, Umam C, Fauzy M, Wibisono Y, Hawa L (2019) Effect of carbonization temperature variations and activator agent types on activated carbon characteristics of sengon wood waste (Paraserianthes falcataria (L.) Nielsen). IOP Confer Ser: Earth Environ Sci 239:012006. https://doi.org/10.1088/1755-1315/239/1/012006

33. Inyinbor AA, Adekola FA, Olatunji GA (2017) Kinetics and isothermal modeling of liquid phase adsorption of rhodamine B onto urea modified Raphia hookerie epicarp. Appl Water Sci 7:3257–3266. https://doi.org/10.1007/s13201-016-0471-7

34. Çelekli A, Bozkurt H, Geyik F (2015) Artificial neural network and genetic algorithms for modeling of removal of an azo dye on walnut husk. Desalin Water Treat 57:15580–15591. https://doi.org/10.1080/19443994.2015.1070759

35. Premkumar Y, Vijayaraghavan K (2015) Biosorption potential of coco-peat in the removal of methylene blue from aqueous solutions. Sep Sci Technol 50:1439–1446

36. Jegan J, Praveen S, Bhagavathi Pushpa T, Gokulan R (2020) Biodecolorization of basic violet 03 using biochar derived from agricultural wastes: isotherm and kinetics. J Biobased Mater Bioenergy 14(03):316–326. https://doi.org/10.1166/jbmb.2020.1969

37. Dutta S, Parsons SA, Bhattacharjee C, Bandyopadhyay S, Datta S (2010) Development of an artificial neural network model for adsorption and photocatalysis of reactive dye on TiO2 surface. Expert Syst Appl 37:8634–8638

38. Ertaş M, Acemioğlu B, Alma MH (2010) Mustafa Usta: Removal of methylene blue from aqueous solution using cotton stalk, cotton waste and cotton dust. JHazard Mater 183:421–427

39. Ai L, Li M, Li L (2011) Adsorption of turquoise blue from aqueous solution with activated carbon/cobalt ferrite/alginate composite beads: kinetics, isotherms, and thermodynamics. J Chem Eng 56:3475–3483

40. Priya AK, Gokulan R, Vijaya Kumar A, Praveen S (2020) Biodecolorization of remazol dyes using biochar derived from Ulva reticulata: isotherm, kinetics, desorption and thermodynamic studies. Desalin Water Treat 200:286–295. https://doi.org/10.5004/dwt.2020.26098

41. Bulut Y, Aydın H (2006) A kinetics and thermodynamics study of turquoise blue adsorption on wheat shells. Desalination 194:259–267

42. Senthilkumaar S, Varadarajan PR, Porkodi K, Subbhuraa CV (2005) Adsorption of turquoise blue onto jute fiber carbon: Kinetics and equilibrium studies, J. Colloid Interface Sc 284:78–82

43. Annadurai G, Juang R-S, Lee D-J (2002) Use of cellulose-based wastes for adsorption of dyes from aqueous solutions. J Hazard Mater 92(263–274):263–274

44. Yu L, Luo Y-M (2014) The adsorption mechanism of anionic and cationic dyes by Jerusalem artichoke stalk-based mesoporous activated carbon. J Environ Chem Eng 2.1(220-229)

45. Zamri MZA, Yahya NY, Ramli RS, Ngadi N, Widia M (2019) Characterization of banana peels waste adsorbent for preliminary study of turquoise blue removal from aqueous solution. Mater Sci Eng 697:1–8

46. Ahmad MA, Eusoff M, Oladoye P, Adegoke KA, Bello O (2020) Statistical optimization of remazol brilliant blue R dye adsorption onto activated carbon prepared from pomegranate fruit peel. Chem Data Collect 28:100426

47. Ahmad MA, Ahmad N, Bello OS (2015) Removal of remazol brilliant blue reactive dye from aqueous solutions using watermelon rinds as adsorbent. J Dispers Sci Technol 36(6):845–858

48. Umoren SA, Etim UJ, Israel AU (2013) Adsorption of turquoise blue from industrial effluent using poly (vinyl alcohol). J Mater Environ Sci 4(1):75–86

49. Dawood S, Sen TK, Phan C (2016) Adsorption removal of turquoise blue (TB) dye from aqueous solution by bio-char prepared from eucalyptus sheathiana bark: kinetic, equilibrium, mechanism, thermodynamic and process design. Desalin Water Treat 57:28964–28980

50. Kocadagistan B, Kocadagistan E (2016) Batch and column removal of the dye blue 3R over pumice. Desalin Water Treat 57:1–14. https://doi.org/10.1080/19443994.2016.1184186

51. Aljeboree A, Alshirifi A, Alkaim A (2014) Kinetics and equilibrium study for the adsorption of textile dyes on coconut shell activated carbon. Arab J Chem 2014:150. https://doi.org/10.1016/j.arabjc.2014.01.020

52. Kumar M, Gokulan R, Sujatha S, Shanmuga Priya SP, Praveen S, Elayaraja S (2021) Biodecolorization of reactive red 120 in batch and packed bed column using biochar derived from Ulva reticulata. Biomass Conv Bioref. https://doi.org/10.1007/s13399-020-01268-x

53. Raman MK, Muthuraman G (2018) Removal of binary mixture of textile dyes on Prosopis juliflora pods - equilibrium, kinetics and thermodynamics studies. Iran J Energy Environ 8(1):48–55. https://doi.org/10.5829/IDOSI.IJEE.2017.08.01.09